Ultrasound-Induced Polymerization of Methyl Methacrylate in Liquid Carbon Dioxide: A Clean and Safe Route to Produce Polymers with Controlled Molecular Weight

Maartje Kemmere, Martijn Kuijpers, Leon Jacobs, Jos Keurentjes*

Process Development Group, Department of Chemical Engineering & Chemistry, Eindhoven University of Technology, P.O. Box 513, 5600 MB Eindhoven, The Netherlands
E-Mail: m.f.kemmere@tue.nl

Summary: Ultrasound-induced cavitation is known to enhance chemical reactions as well as mass transfer at ambient pressures. Ultrasound is rarely studied at higher pressures, since a high static pressure hampers the growth of cavities. Recently, we have shown that pressurized carbon dioxide can be used as a medium for ultrasound-induced reactions, because the static pressure is counteracted by the higher vapor pressure, which enables cavitation. With the use of a dynamic bubble model, the possibility of cavitation and the resulting hot-spot formation upon bubble collapse have been predicted. These simulations show that the implosions of cavities in high-pressure fluids generate temperatures at which radicals can be formed. To validate this, radical formation and polymerization experiments have been performed in CO_2-expanded methyl methacrylate. The radical formation rate is approximately $1.5*10^{14}$ s^{-1} in this system. Moreover, cavitation-induced polymerizations result in high-molecular weight polymers. This work emphasizes the application potential of sonochemistry for polymerization processes, as cavitation in CO_2-expanded monomers has shown to be a clean and safe route to produce polymers with a controlled molecular weight.

Keywords: cavitation; molecular weight distribution; pressurized carbon dioxide; radical polymerization; ultrasound

Introduction

Sonochemistry comprises all chemical and physical effects that are induced by ultrasound. Most of these effects are caused by cavitations, i.e. the collapse of microscopic bubbles in a liquid. The cavities are generated when the negative pressure during the rarefaction phase of the sound wave is sufficiently large to disrupt the liquid. Due to compression of the gas-phase inside the cavity, the implosion of these cavities can locally produce enormous temperatures and pressures (5000 °C, 1000 bar) for very short times[1,2], thus inducing the conditions to perform mechanical work and chemical reactions. The chemical effects of ultrasound include the formation of radicals and

 DOI: 10.1002/masy.200450225

the enhancement of reaction rates at ambient temperatures. The enhanced dissolution of a solid reactant or catalyst caused by renewal of the liquid at the solid-liquid interface illustrates a mechanical effect induced by ultrasound[3].

In ordinary solvents, cavitation does not occur at elevated pressures[4]. As a result, sonochemical studies have been limited to atmospheric conditions. However, in the case of high-pressure fluids, such as liquid carbon dioxide, ethylene and propane, the static pressure is counteracted by the higher vapor pressure, resulting in cavitation and radical formation[5]. Especially the application of liquid carbon dioxide is interesting since it is regarded as an environmentally friendly compound. Additionally, carbon dioxide is non-toxic, non-flammable and naturally abundant.

In this work cavitation effects have been studied at elevated pressure in liquid carbon dioxide and CO_2-expanded methyl methacrylate (MMA). The maximum temperature and bubble wall velocity during collapse have been calculated using a dynamic bubble model for liquid CO_2. To validate these calculations, high-pressure cavitation experiments have been carried out in liquid CO_2. In addition, radical formation experiments and polymerization experiments have been performed to prove the hot-spot formation in CO_2-expanded MMA.

Cavitation bubble dynamics

To initiate the growth of a cavitation bubble, a minimum acoustic pressure has to be applied. The Blake threshold pressure P_B describes this critical pressure[6]. Equation 1 assumes that the static gas pressure (P_0), the vapor pressure (P_v), the surface tension (σ) and the equilibrium radius of the bubble (R_0) determine the required negative pressure in the liquid to start the explosive growth of a cavity.

$$P_B = P_0 - P_v + \frac{4}{3}\cdot\sigma\cdot\sqrt{\frac{2}{3}\cdot\frac{\sigma}{\left(P_0 + 2\cdot\frac{\sigma}{R_0} - P_v\right)\cdot R_0^{\,3}}} \qquad (1)$$

During pressurization of a liquid, the Blake threshold pressure increases, which implies that higher acoustic pressures are needed to produce cavitations. Obviously, no cavitation occurs when the Blake threshold pressure exceeds the maximum acoustic pressure that can be applied.

The Blake threshold describes the onset of the explosive growth of a cavitation bubble. After this, the bubble is no longer static, which requires a dynamic model to calculate the motion of the bubble. In this study the Kyuchi-Yasui model[7] is used to describe the dynamic movement of the bubble. The model is based on the Rayleigh-Plesset equation (equation 2), which includes the density of the fluid (ρ), the gas pressure, the surface tension, the equilibrium radius of the bubble, the vapor pressure, the polytropic index of the gas phase (κ), the liquid viscosity (η) and the acoustic pressure (P_{ac}).

$$R \cdot \frac{d^2}{dt^2} R + \frac{3}{2} \cdot \left(\frac{d}{dt} R \right)^2 = \frac{1}{\rho} \cdot \left(\left(P_0 + \frac{2 \cdot \sigma}{R_0} - P_v \right) \cdot \left(\frac{R_0}{R} \right)^{3 \cdot \kappa} + P_v - \frac{2 \cdot \sigma}{R} - \frac{4 \cdot \eta \cdot \frac{d}{dt} R}{R} - P_0 - P_{ac}(t) \right) \qquad (2)$$

The Rayleigh-Plesset equation is combined with a mass and energy balance over the bubble, which results in a calculated radius of the cavitation bubble as a function of time.

Experimental

Cavitation in liquid-carbon dioxide and the radical formation experiments were studied in a jacketed 175 mL high-pressure vessel, equipped with quartz windows. A schematic drawing of this vessel is given in Figure 1. Sonification of the liquid was performed using 20 kHz ultrasound, which was produced by a Sonics and Materials VC-750 ultrasonic generator. A titanium ½ inch full wave probe was used to couple the piezoelectric transducer to the liquid. The probe was connected to the vessel at its nodes. The temperature inside the vessel was controlled by a heating/cooling bath. A camera in front of the quartz windows was used to observe cavitation events in the high-pressure vessel. Moreover, the light absorption of a radical scavenger was measured by UV-Vis spectroscopy through these windows. The absorption decrease of the active radical scavenger (1,1-diphenyl-2-picrylhydrazyl, DPPH) was used to determine the radical formation rate[8] in CO_2-expanded MMA. The absorption coefficients for the active and inactive radical-scavenger are $8*10^3$ and $2*10^3$ L/(mol cm), respectively. The composition and density of the MMA-CO_2 system is modeled with the Peng-Robinson equation of state and the Panagiotopoulos and Reid mixing rule[9]. The polymerization experiments were performed in a 1.8 L high-pressure reaction calorimeter RC1e (Mettler-Toledo GmbH, HP60 reactor, Switzerland). A detailed description of this equipment is given by Varela de la Rosa et al.[10]

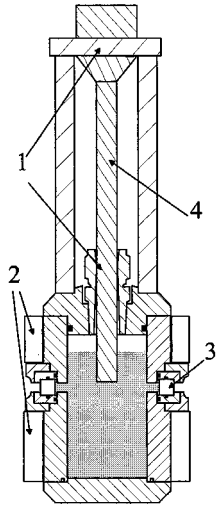

Figure 1. Schematic drawing of the high-pressure vessel (1) attachment points for ultrasound horn (2) cooling/heating jacket, (3) quartz windows, (4) ultrasound horn.

Results and discussion

Bubble dynamics at high pressure

The possibility of ultrasound-induced cavitation and in-situ radical formation in liquid carbon dioxide has been studied. To establish the determining physical properties of high-pressure fluids, the growth and the implosion of a cavity in water and in liquid carbon dioxide have been compared. Since the Blake threshold pressure of liquid carbon dioxide at 58.2 bar equals the threshold pressure of water at 1 bar and 20 °C, 58.2 bar has been used in these calculations.

In Figure 2A the calculated Blake threshold pressure of carbon dioxide and water at 58.2 bar is given as a function of temperature. The threshold curves are calculated using equation 1, in which the vapor pressure is the most important parameter, next to the hydrostatic pressure and the surface tension. For water the Blake threshold is only determined by the static pressure and the surface tension of the liquid, due to the low vapor pressure of water. As the vapor pressure does not change significantly with increasing temperature, the threshold pressure of water is virtually constant. In most liquids a high static pressure hampers the growth of nuclei as a result of the minor influence of the vapor pressure. In the case of carbon dioxide, which condenses at a substantially higher pressure, the vapor pressure does have a significant influence as can be seen

in Figure 2. As a result of this, the Blake threshold pressure is reduced, which enables cavitations in liquid carbon dioxide at higher pressures.

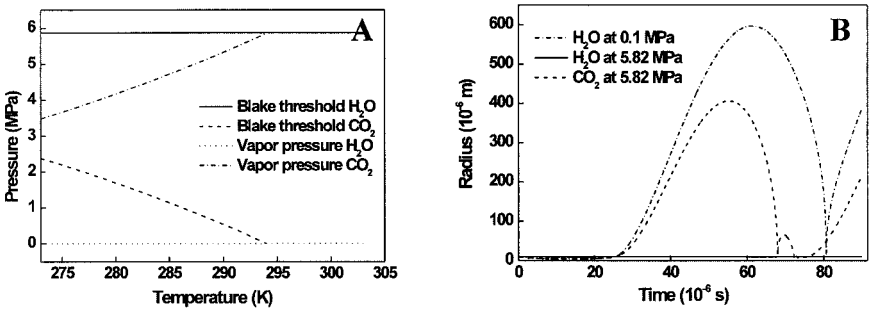

Figure 2. (A) Calculated Blake threshold pressure and vapor pressure for water and CO_2 at 58.2 bar as a function of pressure. (B) Calculated radius of a cavitation bubble as a function of time in water and CO_2.

The dynamic movement of the bubble wall has been calculated using the Kyuchi-Yasui model. Initially, a small cavity with a radius of 10^{-5} m is present, which consists of argon and the corresponding vapor of the liquid phase. In the simulations, an ultrasound wave with an acoustic pressure of 10 bar and a frequency of 20 kHz is imposed on this bubble. The variation of the radius of the bubble is shown in Figure 2B. As the acoustic pressure for water at 58.2 bar is lower than the Blake threshold pressure, almost no bubble movement is observed and no cavitation can occur. In contrast to the situation in water, carbon dioxide at 58.2 bar allows for cavitation and the bubble exhibits a similar movement compared to water at 1 bar. Moreover, the maximum temperature (585 K) and maximum bubble wall velocity (777 m/s) reached during collapse in liquid CO_2 are in the same order of magnitude as compared to water at ambient pressure (722 K and 840 m/s).

Cavitation and radical formation at high pressure

Figure 3 indicates that experiments in the high-pressure vessel show that the required threshold pressure can easily be exceeded at a relatively low acoustic pressure for liquid CO_2 (10°C, 75 bar), proving the influence of the vapor pressure in the Blake threshold calculations and the dynamic simulations.

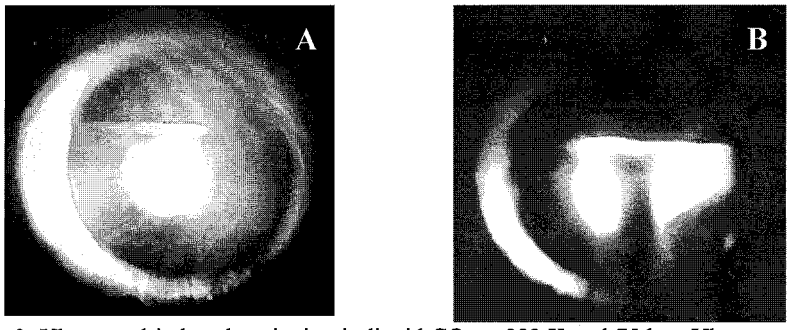

Figure 3. Ultrasound-induced cavitation in liquid CO_2 at 283 K and 75 bar. Ultrasound intensity of 25 W/cm^2 (A) and 125 W/cm^2 (B). In (A), no cavitation occurs and the liquid remains transparent, whereas in (B) indeed cavitation occurs, visible by the presence of dispersed gas bubbles underneath the ultrasound horn. Additionally, the cavitation threshold can simply be determined by ear.

To show that bubble collapse in liquid CO_2 is sufficiently strong to induce radical formation, UV-Vis measurements have been carried out using the radical scavenger DPPH in CO_2-MMA systems at high pressure. In Figure 4A, a decrease in the absorption of the radical scavenger during sonification is shown, indicating that radicals are produced. The radical formation rate is approximately $1.5*10^{14}$ s^{-1}, for which no noticeable difference between the three systems is observed (Figure 4B). An extra head-pressure is added, to determine its influence on cavitation and to prevent boiling. Which occurs at a molar fraction CO_2 of 0.64 without argon.

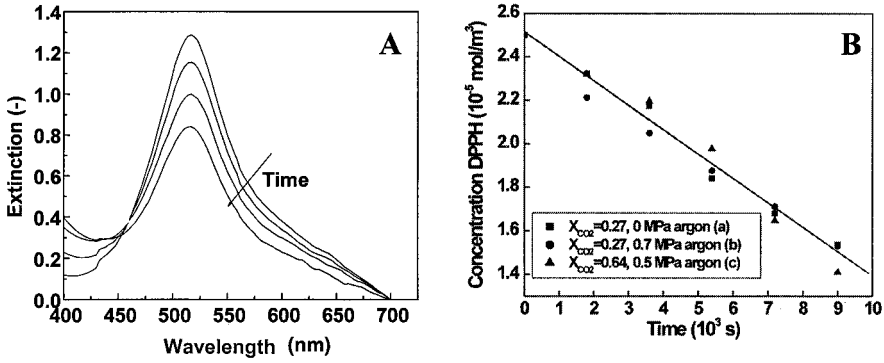

Figure 4. (A) UV-Vis spectra of DPPH in time for CO_2-MMA (0.23-0.73) under sonification at 20 °C. (B) Concentration of DPPH in time as determined by UV-Vis analysis at 520 nm, for three different systems at 20 °C.

Ultrasound-induced precipitation polymerization in CO_2-expanded MMA

Since the radicals are generated in-situ by ultrasound, no initiator or catalyst is required to perform an ultrasound-induced polymerization. An additional advantage of this technique is the intrinsic safe operation, because turning off the electrical power supply will immediately stop the radical formation and consequently the polymerization reaction. However, ultrasound-induced *bulk* polymerization is limited to relative low conversions, because the formed *dissolved* polymer chains cause a drastic increase in the viscosity, resulting in slower growth and collapse of the cavity. Since the cavitations become less effective, the radical formation rate will decrease. Typically, an ultrasound-induced *bulk* polymerization has a maximum conversion of approximately 15%[11], because the collapse is no longer sufficiently strong to induce hot-spot temperatures that are able to generate radicals. In order to obtain higher conversions, *precipitation* polymerization forms a solution because the produced polymer precipitates from the reaction medium. As a result, the radical formation rate is expected to remain virtually constant. In this perspective, liquid carbon dioxide is a suitable medium as most monomers have a high solubility in CO_2, whereas it exhibits an anti-solvent effect for most polymers. In this study polymerization experiments have been performed in the previously described CO_2-MMA systems, now without the radical scavenger DPPH.

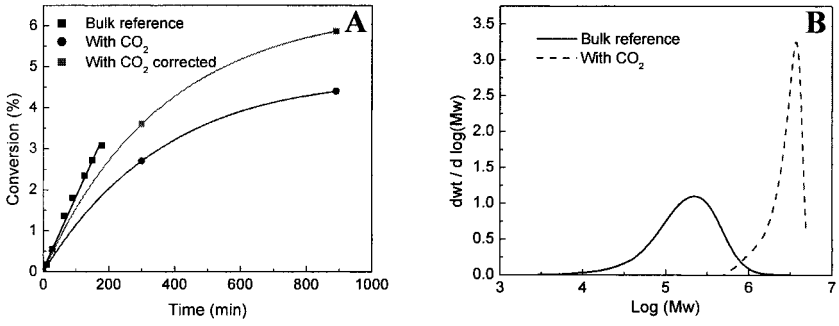

Figure 5. (A) Conversion-time history of ultrasound-induced polymerization of MMA (B) Resulting molecular weight distributions.

Figure 5A shows the conversion time history of ultrasound-induced polymerization of MMA at 6 bar CO_2 pressure (mole fraction CO_2 = 0.28), constructed from two separate experiments. To compare the results with a reference experiment performed in bulk MMA at ambient pressure, a correction for the lower MMA-concentration has to be made (original conversion values divided by the mole fraction MMA, i.e. 0.72). Both the polymerization in CO_2 and the bulk experiment at ambient pressure appear to have the same order of magnitude in reaction rate. Although the viscosity does not increase during the precipitation polymerization (see the next alinea), so far only relatively low conversions have been obtained (7%). This is a result of the large reactor scale compared to the ultrasound power input to the system. As soon as the reactor and ultrasound power are better scaled, it is expected that high conversions will be reached.

Figure 5B indicates that in the CO_2-system a precipitated polymer has been obtained with a much higher molecular weight (>10^7g/mol, beyond GPC measurement) as compared to a reference experiment performed in bulk MMA at ambient pressure (10^5g/mol). A possible explanation for the difference in molecular weight is the fact that a precipitated polymer is not susceptible to ultrasound-induced polymer scission (see the next paragraph), whereas the dissolved polymer chains in the bulk experiment can break due to cavitation. In addition, it is possible that the precipitated polymer chains are swollen with monomer and continue to grow, while termination is not likely to occur in that particular situation.

During the polymerizations, the overall heat transfer coefficient (U) was continuously being calculated using temperature oscillation calorimetry [12,13]. Several resistances in series determine the value of U as illustrated by equation 3.

$$\frac{1}{U_i} = \frac{1}{h_i} + \frac{D_i}{2k_w} \ln\frac{D_0}{D_i} + \frac{1}{h_0}\frac{D_i}{D_0} \qquad (3)$$

In equation 3 the heat transfer coefficient is based on the inside area, for which h_i and h_o represent the partial heat transfer coefficient in the vessel and the jacket, respectively; k_w stands for the thermal conductivity coefficient of the wall; D_i and D_o are the inner and outer diameter of the vessel.

The last two terms of equation 3 remain constant during the polymerization, because the

properties of the reactor wall and cooling liquid will not change during the experiments. Therefore, U provides an indirect measure of the viscosity of the reaction mixture, since the empirical relation for the Nusselt number as a function of the Reynolds and Prandtl number can be applied to couple h_i to the viscosity[14]. Figure 6 shows that the reference experiment in bulk MMA at ambient pressure exhibits a strong decrease of the heat-transfer coefficient, indicating a significant viscosity increase whereas the polymerization performed in CO_2-expanded MMA at 293K and 6 bar shows a minor viscosity increase up until a conversion of 5%. In the polymerization with 6 bar CO_2 pressure, carbon dioxide acts as an anti-solvent, thus enabling a viscosity reduction, because the gyration radius of a polymer is smaller when an anti-solvent is present. Additionally, a low solvent viscosity will be maintained at higher conversions, as the polymer will precipitate from the solution.

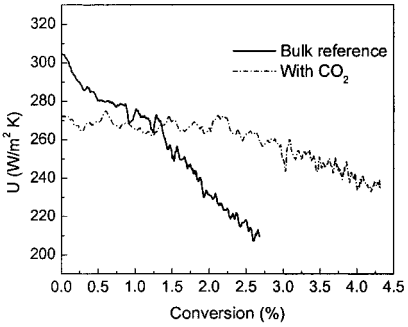

Figure 6. Overall heat transfer coefficient as calculated by temperature oscillation calorimetry.

Control of molecular weight by polymer scission and precipitation

In terms of product properties, the molecular weight distribution (MWD) is an important characteristic of polymers. In industry, often a post-processing step is applied to alter the MWD of the polymers, e.g. peroxide-induced degradation of polyolefins[15]. Since cavitation can induce chain scission as well, ultrasound can be applied as an alternative method.

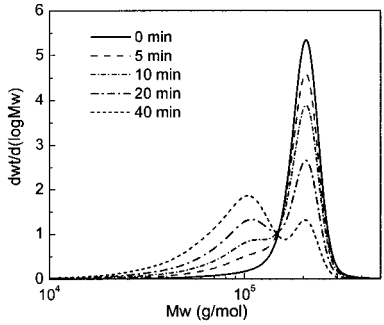

Figure 7. Ultrasound-induced polymer scission of 0.1 wt% PMMA in MMA, a small amount of DPPH was added to ensure no reaction or recombination of polymeric radicals could occur.

This mechanism is similar to flow-induced chain scission. Due to the forces exerted on the polymer, ultrasound-induced chain breakage occurs exactly in the middle[16], see Figure 7. Depending on the ultrasound intensity and viscosity of the solution, the molecular weight of the polymer product can be limited to 30.000 g/mol. This concept provides an additional means to control the molecular weight of the product by either polymer scission or precipitation. At high monomer-CO_2 ratios most polymer chains are dissolved in the reaction mixture and will be susceptible to cavitation-induced polymer scission, whereas at low monomer-CO_2 ratios, carbon dioxide will act as an antisolvent inducing polymer precipitation. Although cavitation occurs in the reaction mixture, the precipitated polymer will not break and will maintain a high molecular weight.

Conclusion

Ultrasound has been applied to create cavitation in pressurized CO_2. The Blake threshold pressure for cavitation can be exceeded at a relatively low acoustic intensity, because the hydrostatic pressure is counteracted by the high vapor pressure of carbon dioxide. Using a dynamic bubble model, the formation of hot spots upon bubble collapse is predicted. This hot-spot formation has experimentally been confirmed by radical formation and polymerization experiments in CO_2-expanded MMA. During the polymerization reactions, carbon dioxide acts as an anti-solvent and precipitates the polymer. This enables a viscosity reduction during ultrasound-induced polymerization in CO_2 –MMA systems as compared to polymerizations in bulk MMA at ambient

pressure, which in principle allows reaching high conversions. Moreover, tuning the monomer-CO_2 ratio enables control over molecular weight by either polymer scission or polymer precipitation.

[1] K.S. Suslick, *Sci. Am.*, **1989**, *260*, 80.
[2] J.-L. Luche, "*Synthetic Organic Sonochemistry*", Plenum, New York, 1998.
[3] L.H. Thompson, L.K. Doraiswamy, *Ind. Eng. Chem. Res.*, **1999**, *38*, 1215.
[4] J. Berlan, F. Trabelsi, H. Delmas, A.M. Wilhelm, J.F. Petrignani, *Ultrason. Sonochem.*, **1994**, *1*, S97.
[5] M.W.A. Kuijpers, D. van Eck, M.F. Kemmere, J.T.F. Keurentjes, *Science*, **2002**, *298*, 1969.
[6] T.J. Leighton, "*The Acoustic Bubble*", Academic Press, London, 1998, p 86.
[7] K. Yasui, *J. Acoust. Soc. Am.*, **1995**, *98*, 2772.
[8] M.W.A. Kuijpers, M.F. Kemmere, J.T.F. Keurentjes, *Ultrasonics*, **2002**, *40*, 675.
[9] M.F. Kemmere, M.H.W. Cleven, M.A. van Schilt, J.T.F. Keurentjes, *Chem. Eng. Sci.*, **2002**, *57*, 3929.
[10] L. Varela de la Rosa, E.D. Sudol, M.S. El-Aasser, A. Klein, *J. Polym. Sci.*, **1996**, *34*, 461.
[11] G.J. Price, *Ultrason. Sonochem.*, **1996**, *3*, S229.
[12] R. Carloff, A. Proβ, K.-H. Reichert, *Chem. Eng. Tech.*, **1994**, *17*, 406.
[13] A. Tietze, A. Proβ, K.-H. Reichert, *DECHEMA Monogr.*, **1995**, *131*, 673.
[14] M.F. Kemmere, J. Meuldijk, A.A.H. Drinkenburg, A.L. German, *Polymer Reaction Engineering*, **2000**, *8*, 271.
[15] A.V. Machado, J.A. Covas, M. van Duin, *J. Applied Polym. Sci.*, **2001**, *81*, 1, 58.
[16] M.W.A. Kuijpers, P.D. Iedema, M.F. Kemmere, J.T.F. Keurentjes, submitted.